

## Article

# Near-Infrared Spectroscopy Study of Serpentine Minerals and Assignment of the OH Group

Shaokun Wu <sup>1,\*</sup>, Mingyue He <sup>1,\*</sup>, Mei Yang <sup>2</sup>, Biyao Zhang <sup>1</sup>, Feng Wang <sup>3</sup> and Qianzhi Li <sup>3</sup>

<sup>1</sup> Gemological Institute, China University of Geosciences, Beijing 100083, China; 3009210005@email.cugb.edu.cn (S.W.); zhangby889@163.com (B.Z.)

<sup>2</sup> Sciences Institute, China University of Geosciences, Beijing 100083, China; yangmei@cugb.edu.cn

<sup>3</sup> Shaanxi Mine in Hanyuan Jade Industry Co., Ltd., Hanzhong 723000, China; wang13891685963@163.com (F.W.); qianzhili2021@163.com (Q.L.)

\* Correspondence: hemy@cugb.edu.cn

**Abstract:** Three different kinds of serpentine mineral samples were investigated using Fourier transform near-infrared spectroscopy (FTNIR). The results show that there are obvious differences in the characteristic infrared spectra of the three serpentine group minerals (lizardite, chrysotile, and antigorite), which can easily be used to identify these serpentine minerals. The combination of weak and strong peaks in the spectrum of lizardite appears at 3650 and 3690  $\text{cm}^{-1}$ , while the intensities of the peaks at 4281 and 4301  $\text{cm}^{-1}$  (at 7233 and 7241  $\text{cm}^{-1}$ , respectively) are similar. A combination of weak and strong peaks in chrysotile appears at 3648 and 3689  $\text{cm}^{-1}$  and at 4279 and 4302  $\text{cm}^{-1}$ , and a single strong peak appears at 7233  $\text{cm}^{-1}$ . In antigorite, there are strong single peaks at 3674, 4301, and 7231  $\text{cm}^{-1}$ , and the remaining peaks are shoulder peaks or are not obvious. The structural OH mainly appears as characteristic peaks in four regions, 500–720, 3600–3750, 4000–4600, and 7000–7600  $\text{cm}^{-1}$ , corresponding to the OH bending vibration, the OH stretching vibration, the OH secondary combination vibration, and the OH overtone vibration, respectively. In the combined frequency vibration region, the characteristic peak near 4300  $\text{cm}^{-1}$  is formed by the combination of the internal and external stretching vibrations and bending vibrations of the structural OH group. The overtone vibrations of the OH stretching vibration appear near 7200  $\text{cm}^{-1}$ , and the practical factor is about 1.965. The near-infrared spectra of serpentine minerals are closely related to their structural differences and isomorphous substitutions. Therefore, near-infrared spectroscopy can be used to identify serpentine species and provides a basis for studies on the genesis and metallogenic environment of these minerals.

**Keywords:** near-infrared spectroscopy; lizardite; chrysotile; antigorite; OH group



**Citation:** Wu, S.; He, M.; Yang, M.; Zhang, B.; Wang, F.; Li, Q. Near-Infrared Spectroscopy Study of Serpentine Minerals and Assignment of the OH Group. *Crystals* **2021**, *11*, 1130. <https://doi.org/10.3390/cryst11091130>

Academic Editors: Sergey V. Krivovichev, Taijin Lu, Fei Liu and Tingting Gu

Received: 27 July 2021

Accepted: 12 September 2021

Published: 17 September 2021

**Publisher's Note:** MDPI stays neutral with regard to jurisdictional claims in published maps and institutional affiliations.



**Copyright:** © 2021 by the authors. Licensee MDPI, Basel, Switzerland. This article is an open access article distributed under the terms and conditions of the Creative Commons Attribution (CC BY) license (<https://creativecommons.org/licenses/by/4.0/>).

## 1. Introduction

Infrared spectroscopy can be a powerful tool for identifying compounds, crystal structure and isomorphism. In geology, mid-infrared and near-infrared spectroscopy are commonly used for research. Mid-infrared (MIR) generally refers to the infrared spectrum in the range 400–4000  $\text{cm}^{-1}$  (2.5–2.5  $\mu\text{m}$ ). Among them, the 1500–4000  $\text{cm}^{-1}$  region can identify the characteristic fundamental frequency vibration of some groups. The 400–1500  $\text{cm}^{-1}$  region is called the “fingerprint area” [1], which can identify specific molecular structure from their spectrum. The near-infrared spectrometer was available as early as the 1920s, long before the popularization of the mid-infrared spectrometer laboratory [2]. Near-infrared (NIR) generally refers to the infrared spectrum in the range 4000–12,500  $\text{cm}^{-1}$  (2.5–1  $\mu\text{m}$ ). It has been widely used in agriculture, the chemical industry, and other fields due to its fast and non-destructive characteristics [3–6]. In geology, near-infrared spectroscopy mainly reflects the combination bands and overtone bands of water or different functional groups in minerals structure, as well as the combination modes of the hydroxyl group and metal ions, which can reflect the differences in the composition

and structure of minerals. Therefore, it is very useful for the identification and study of minerals.

Serpentine minerals are trioctahedral phyllosilicates type 1:1 and consist of  $\text{SiO}_4$  tetrahedral sheets and octahedral brucite-like sheets. They produce different structures because of the lattice mismatch between the octahedral (O) and the tetrahedral (T) sheets. The compensation for this mismatch occurs through chemistry changes or through curvature of the layers [7]. Based on these different structures, serpentine can be divided into three types: lizardite, antigorite, and chrysotile. Lizardite has a flat crystal structure, where the planar sheet presents an ideal layer topology. Antigorite shows a corrugated wavy layer characterized by a modulated structure. Chrysotile with the cylindrical spiral wrapping of the 1:1 layer exhibits a fibrous structure. Naturally occurring intergrowths of the three types of serpentine minerals are very common. Among the conventional techniques used to identify serpentine minerals without losing microstructural information, only Transmission Electron Microscopy with EDS (TEM-EDS) gives unambiguous results; however, sample preparation is complex and time-consuming, and the interpretation of the electron diffraction patterns is not easy [8]. Therefore, it is necessary to find a simple characterization technique to identify and distinguish between these three minerals.

Infrared spectroscopy is a powerful tool for quickly identifying different types of clay minerals. The IR spectra of phyllosilicates have been summarized by Farmer [9]. Serpentes exhibit  $\nu\text{OH}$  (OH-stretching) bands in the range  $3650\text{--}3700\text{ cm}^{-1}$  and  $\delta\text{OH}$  (OH-vibrating) bands near  $618$  and  $646\text{ cm}^{-1}$ , due to their inner and surface hydroxyls [9]; however, there is no specific distinction between the peaks of the inner and surface hydroxyl groups. Cheng et al. [10] measured and distinguished five phyllosilicate minerals using near-infrared spectroscopy, including pyrophyllite, muscovite, talc, chrysotile, and kaolinite. Li et al. [11] analyzed the near-infrared spectra of different types of silicate minerals and concluded that there were different types of combined frequency and double-frequency peaks for water in gem minerals. Zhang et al. [12] compared TO- and TOT-type layered silicates and found that layered silicates have a long hydrogen bond, which widens the stretching vibration band of O-H, shifts the band in the direction of the long wave, and sometimes causes double-peak phenomenon to appear. The stretching frequency of the hydroxyl group is also affected by the octahedral cation coordinated with the hydroxyl group.

The purpose of this study is to demonstrate the differences in the near-infrared spectra of three types of serpentines and to discuss the assignments of the major near-infrared bands, which can be used to quickly identify and distinguish between serpentine group minerals. The results of this study are applicable to the identification and research of jewelry, jade, and cultural relics. In addition, the attribution of the OH group's vibration spectrum peak is discussed in detail, which is applicable to investigations of the metallogenic environments and compositional differences of serpentine. Finally, careful measurements and thoughtful interpretations of the infrared spectra of clay minerals may be critical to the interpretation of remotely sensed data from the Earth and Mars.

## 2. Materials and Methods

The experimental samples were divided into three groups according to their mineral type. The lizardite and chrysotile (asbestos) samples were from the Hanzhong area, Shaanxi Province, China; the antigorite samples were from the Xiuyan area, Liaoning Province, China. The refractive index of each sample was between 1.55 and 1.56; the specific gravity was between 2.56 and 2.61. Typical mineral samples were selected from the three groups for this study. The uniform part of each sample, without other phases, was used for the experiments.

SEM-EDS analyses of the serpentine samples before this study showed all samples contain the isomorphic element iron, which is very common in serpentine minerals. There are few other kinds of isomorphic elements (Table 1).

**Table 1.** Mineral composition of the samples.

Samples	Minerals	Form	Color	Isomorphism
DWH14-lz	Lizardite	Block	Yellow	Fe/0.7%, Al/0.1%
ZH41-lz		Block	Brownish yellow	Fe/0.9%
Z3-lz		Block	Brown	Fe/1.0%, Mn/0.1%, Al/0.1%
SZ17-lz		Block	Dark brown	Fe/0.8%, Mn/0.2%, Al/0.1%
SM-ctl	Chrysotile	Fiber	Brown	Fe/0.7%, Mn/0.1%, Al/0.2%
H7-atg	Antigorite	Block	Light yellow	Fe/0.4%, Al/0.1%
H11-atg		Block	Colorless	Fe/0.3%

The X-ray diffraction (XRD) data were acquired using the SmartLab X-ray powder diffractometer at the Institute of Earth Science, China University of Geosciences, Beijing (CUGB). The system was equipped with a conventional copper target X-ray tube (set to 45 kV and 200 mA) and a graphite monochromator, with a stepping-scanning mode with a scanning speed of 4°/min and a step length of 0.02° in the range 3–90°. The testing temperature was 15 °C and the humidity was 22%. The samples were pulverized to 200 mesh powders using an agate mortar and stored immediately in a plastic bag to minimize contamination and oxidation. The results were normalized and analyzed using the MDI Jade 6.5 software and the International Center of Diffraction Database (ICDD).

The Fourier transform near-infrared spectroscopy (FTIR) measurements were performed using the Bruker Tensor II spectrometer at the National Infrastructure of Mineral, Rock, and Fossil Resources for Science and Technology (NIMRF). The spectra were collected in the frequency ranges of 400–4000 cm<sup>-1</sup> (MIR) and 4000–10,000 cm<sup>-1</sup> (NIR) using the KBr compression transmission method, with a resolution of 4 cm<sup>-1</sup>, and 64 scans were accumulated to improve the signal to noise ratio. The testing temperature range was 10–23 °C, and the humidity was less than 22%. The NIR data were processed by baseline removal and normalization.

The regions of 520–700 cm<sup>-1</sup> and 3600–3800 cm<sup>-1</sup> in the mid-infrared (MIR) were complex and the PeakFit v4.12 software was used to fit the peaks in order to find the exact locations of their component peaks. All of the spectra were fitted using a combined Gauss–Lorentz Area function, with  $r^2 > 0.99$ .

### 3. Results

#### 3.1. X-ray Diffraction

The XRD patterns of the seven selected serpentine minerals with standard XRD patterns are shown in Figure 1. The samples DWH14-lz, ZH-41-lz, Z-3-lz, and SZ-17-lz have patterns identical to that of PDF 86-0403, strong peaks at  $d_{(001)} = 12.079$ – $12.099^\circ$  and  $d_{(002)} = 24.301$ – $24.340^\circ$  and medium intensity peaks at  $d_{(-1-11)} = 35.861$ – $35.919^\circ$ , which is the characteristic pattern of lizardite-1T. The sample SM-ctl has a pattern identical to that of PDF 27-1275, showing strong peaks at  $d_{(002)} = 12.020^\circ$  and  $d_{(004)} = 24.300^\circ$ , which is the characteristic pattern of chrysotile. The pattern has fewer but wider peaks and the shape of the peak at  $d_{(020)} = 19.500^\circ$  is asymmetric. The samples H7-atg and H11-atg have patterns identical to that of PDF 07-0417, which is the characteristic pattern of antigorite. The patterns are clear and strong (the weak peak is not obvious after normalization), with strong peaks at  $d_{(001)} = 12.159$ – $12.160^\circ$  and  $d_{(002)} = 24.580$ – $24.599^\circ$ . There is a double peak near  $d_{(-131)} = 35.500$ – $35.520^\circ$  and  $d_{(211)} = 37.022$ – $37.043^\circ$ . All of the samples were found to be almost pure minerals without any other phases.

#### 3.2. Characteristics of MIR

In the mid-infrared range, there are four main spectral bands: 400–500 cm<sup>-1</sup>, 520–700 cm<sup>-1</sup>, 850–1100 cm<sup>-1</sup>, and 3600–3800 cm<sup>-1</sup>. The position, intensity, and number of spectral peaks are very consistent with the standard spectra of serpentine minerals (Figure 2), and no additional peaks appear, indicating that all of the samples are mainly composed of serpentine minerals.

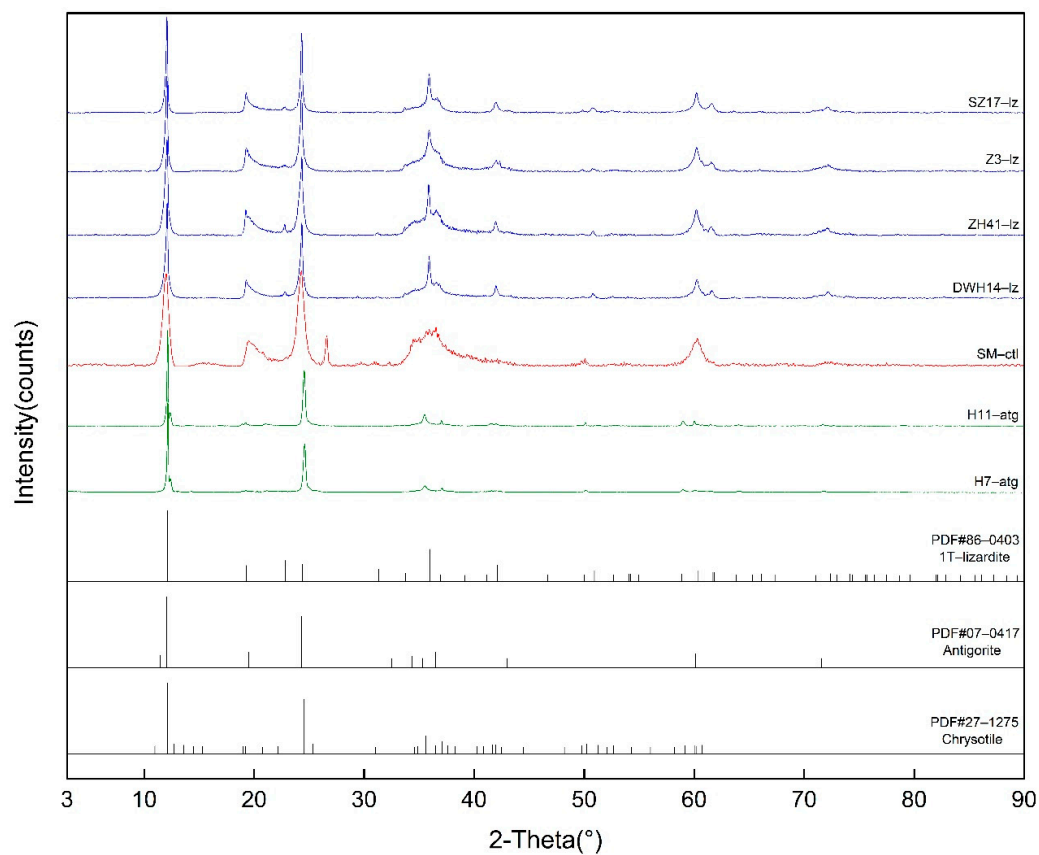


Figure 1. Powder XRD patterns of the samples.

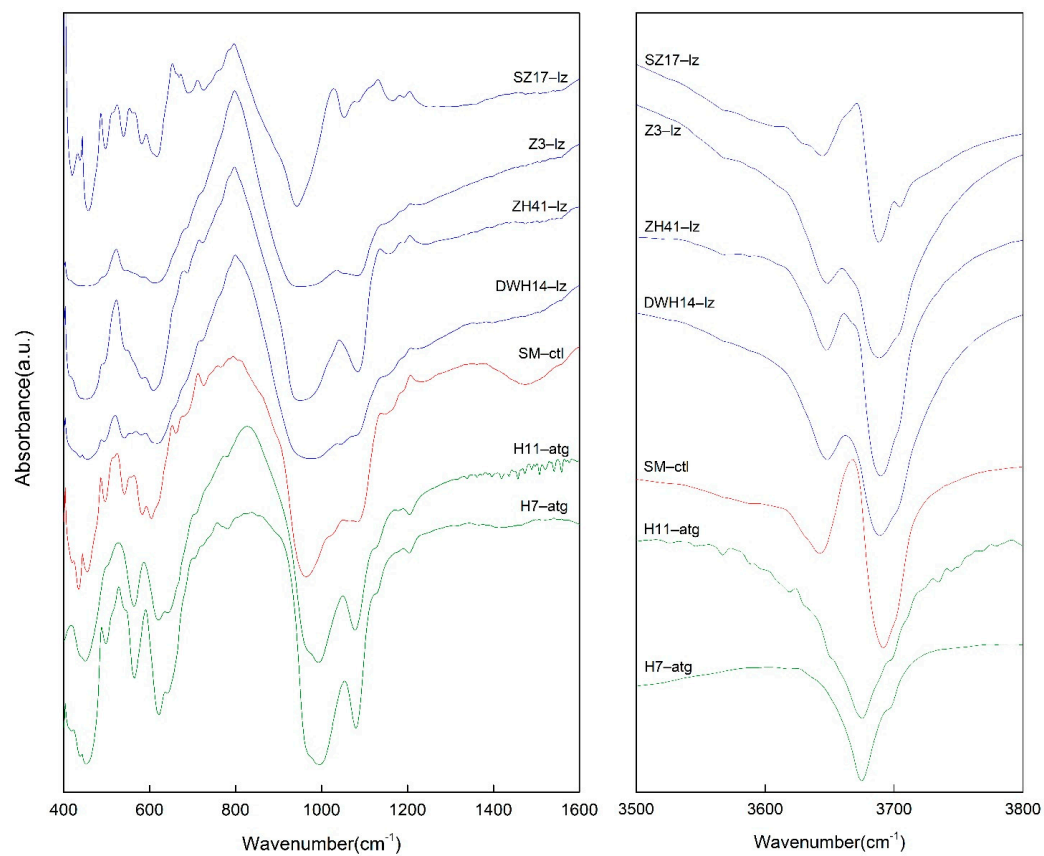
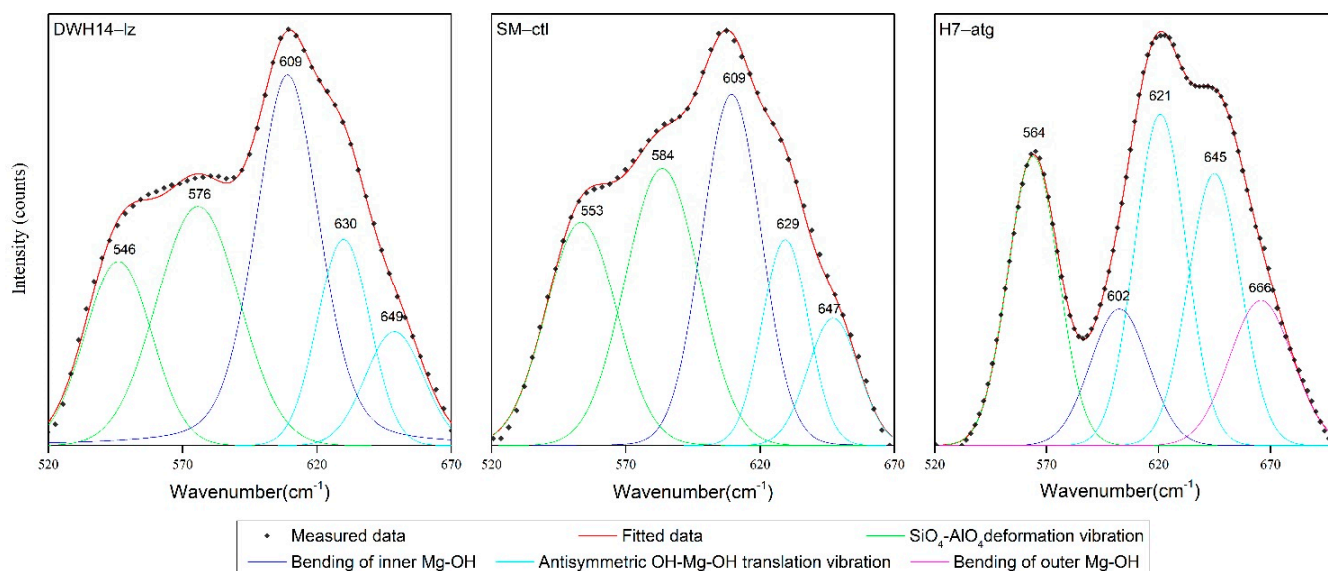


Figure 2. MIR spectra of the serpentinite samples.

There are five peaks in the range 520–700  $\text{cm}^{-1}$ . The spectra of DWH14-lz, ZH41-lz, Z3-lz, SZ17-lz and SM-ctl are similar, with two peaks related to  $\text{SiO}_4$  tetrahedral deformation vibration near 550 and 580  $\text{cm}^{-1}$  and the strongest peak near 609  $\text{cm}^{-1}$ . There is only one absorption peak at 564  $\text{cm}^{-1}$  for H7-atg and H11-atg, and there is a new peak at 666  $\text{cm}^{-1}$ , which is different from the other five samples. The bending and translation vibration peaks of OH in antigorite are generally four to ten wavenumbers lower than those for lizardite and chrysotile.

The peaks in the range of 3600–3800  $\text{cm}^{-1}$  are usually attributed to OH stretching vibrations. The outer sloping OH stretching vibration of the serpentine minerals is at about 3650  $\text{cm}^{-1}$  and the vertical stretching vibration of the outer OH group is around 3670 and 3690  $\text{cm}^{-1}$  [13–16]. Antigorite has a unique small peak at 3632  $\text{cm}^{-1}$  and the stretching vibration of the inner OH group near 3700  $\text{cm}^{-1}$  is not present. This may be due to the periodically symmetric structure, which causes the inner OH vibrations to cancel each other.

Bishop [17] reported that the center of the OH bending vibrations were located at 606  $\text{cm}^{-1}$  for chrysotile and at 625  $\text{cm}^{-1}$  for lizardite. After fitting the peaks, it was found that the vibration peaks of the OH groups in the three types of serpentines were similar, with peaks at 609, 630, and 649  $\text{cm}^{-1}$ , but their strengths varied significantly. Figure 3 shows DWH14-lz, SM-ctl, and H7-atg as representative examples (the other samples have similar patterns). The inner OH bending vibration centers of lizardite and chrysotile are around 609  $\text{cm}^{-1}$ , 630  $\text{cm}^{-1}$ , and 649  $\text{cm}^{-1}$ , which are assigned to the OH translational vibration mode. In the range of OH stretching, for antigorite, the peak at 3674  $\text{cm}^{-1}$  is stronger than the peak at 3693  $\text{cm}^{-1}$ , which are both assigned to the outer OH vertical stretching vibration. The opposite relationship occurs for those peaks in lizardite and chrysotile. Antigorite also lacks the peak near 3700  $\text{cm}^{-1}$  that is assigned to the inner OH stretching vibration. Figure 4 shows DWH14-lz, SM-ctl, and H7-atg as representative examples (the other samples have similar patterns). The detailed peak positions and band assignments of the samples are presented in Table 2.



**Figure 3.** Band component analysis of the 520–700  $\text{cm}^{-1}$  region with DWH14-lz as example of lizardite, SM-ctl as example of chrysotile, and H7-atg as example of antigorite.

### 3.3. Characteristics of NIR

Serpentine minerals have multiple secondary combination bands in the range 4000–4500  $\text{cm}^{-1}$ , with the strongest peak near 4280–4300  $\text{cm}^{-1}$  (Figure 5a). The band centers are listed in Table 3. The results show that lizardite exhibits equal-strength double

peaks near 4280 and 4301  $\text{cm}^{-1}$ . The 4304  $\text{cm}^{-1}$  peak of chrysotile is stronger, and the 4279  $\text{cm}^{-1}$  peak appears as a shoulder. Antigorite has a weaker shoulder peak at 4279  $\text{cm}^{-1}$ , and a new shoulder peak appears at 4315  $\text{cm}^{-1}$ .

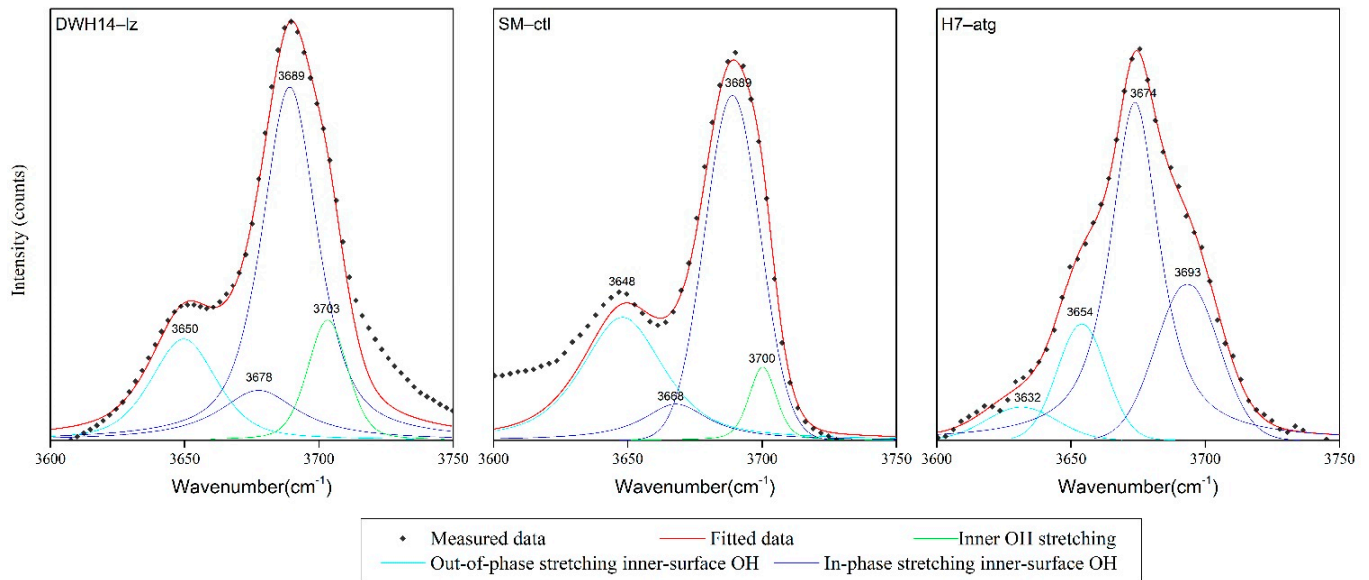


**Figure 4.** Band component analysis of the 3600–3750  $\text{cm}^{-1}$  region with DWH14-lz as example of lizardite, SM-ctl as example of chrysotile, and H7-atg as example of antigorite.

**Table 2.** The MIR bands related to the serpentinite samples and their assignments (in  $\text{cm}^{-1}$ ).

Band Assignment [14,18–23]	DWH14-lz	ZH41-lz	Z3-lz	SZ17-lz	SM-ctl	H7-atg	H11-atg
Antisymmetric Mg-OH translation	441	441	438	438	435	436	435
Mg-OH translation + $\nu_6(e)$ $\text{SiO}_4$	462	462	463	463	454	449	449
$\text{SiO}_4\text{-AlO}_4$ deformation vibration	546	553	551	553	553	564	564
Bending of inner Mg-OH	576	580	580	583	584	666	666
Bending of outer Mg-OH	609	609	609	610	609	602	600
Antisymmetric OH-Mg-OH translation vibration	630	630	629	630	629	621	619
Bending of inner Mg-OH	649	648	646	649	647	645	644
Si-O stretching vibration	961	962	963	956	963	970	969
Si-O <sub>b</sub> -Si stretching vibration	1022	1022	1024	1018	1026	994	993
Si-O <sub>nb</sub> stretching vibration	1080	1078	1080	1079	1080	1080	1077
Outer OH sloping stretching vibration	3650	3647	3649	3648	3648	3654	3653
Outer OH vertical stretching vibration	3678	3665w	3670w	3667	3668	3674	3674
Inner OH stretching vibration	3689	3688	3688	3688	3689	3693	3696
Inner OH stretching vibration	3703	3704	3705	3705	3700		

All of the spectra have a large number of disordered but clear peaks in the ranges 5100–5500  $\text{cm}^{-1}$  and 7000–7500  $\text{cm}^{-1}$  (Figure 5b). Bishop [24] suggested that these bands are probably due to a small amount of  $\text{H}_2\text{O}$  molecules trapped at grain boundaries or are associated with impurities in the samples. However, our experimental results show that the peak position does not shift due to the influence of the type of serpentinite and contents of the impurities. Thus, it is unlikely to be caused by isomorphism and is likely related to the water in the crystal structure. Cheng [10] pointed out that the unbound water in the interlayer structure of clay minerals causes a series of absorption peaks near 5260  $\text{cm}^{-1}$  and 7150  $\text{cm}^{-1}$ , which are generally not assigned. There is a broad absorption band at 5000–5300  $\text{cm}^{-1}$  in chrysotile, which is reported to be caused by a large amount of adsorbed

water in the tubular structure. A similar broad absorption band was observed in the range of 3300–3500  $\text{cm}^{-1}$ .

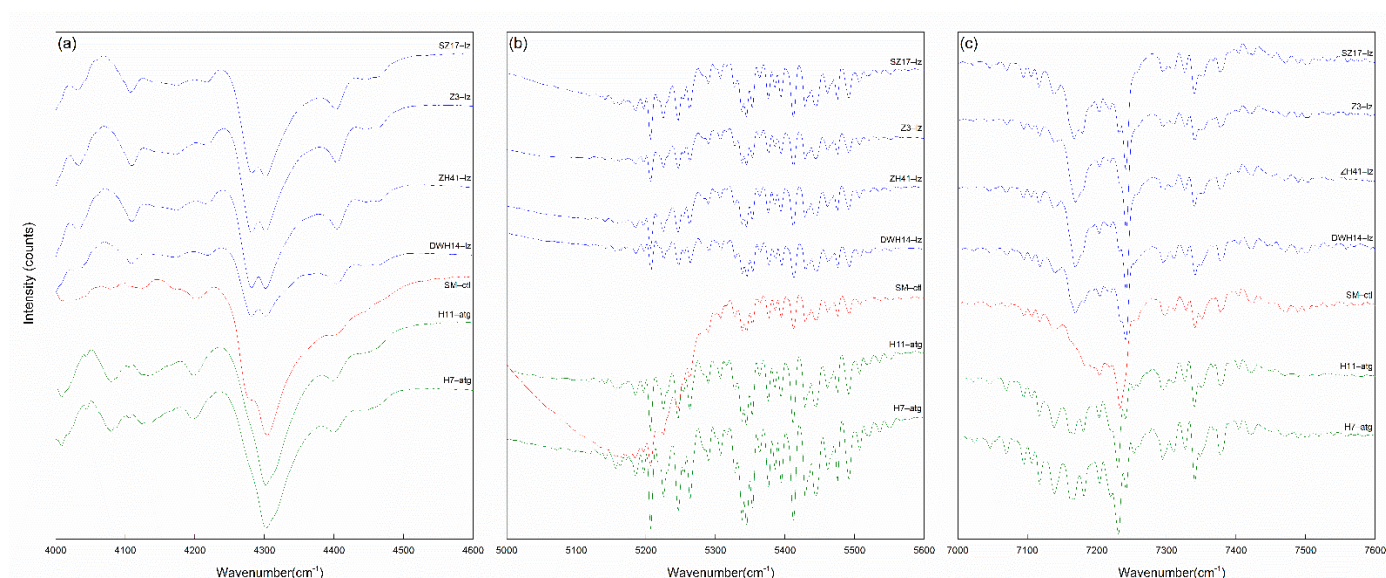


**Figure 5.** NIR spectra of the serpentine samples. (a) Range of the OH-combination bands (4000–4600  $\text{cm}^{-1}$ ); (b) adsorbed water bands (5000–5600  $\text{cm}^{-1}$ ); (c) range of the OH-stretching overtone bands (7000–7600  $\text{cm}^{-1}$ ).

**Table 3.** The bands in the range 4000–4600  $\text{cm}^{-1}$  for the related samples (in  $\text{cm}^{-1}$ ).

J. L. Post [18]	Baron [19]	DWH14-lz	ZH41-lz	Z3-lz	SZ17-lz	SM-ctl	H7-atg	H11-atg
4010	4001	4009	4009	4009	4009	4009	4009	4009
							4044	4043
4076	4077					4078	4079	4079
4123	4121	4109	4109	4109	4108	4106	4105	4105
4196	4199	4218	4218	4218	4218	4201	4197	4197
4279	4274	4281	4281	4281	4281	4279	4279	4279
4303	4307	4301	4301	4301	4301	4304	4302	4301
4315							4315	4315
4401	4409	4404	4404	4404	4404	4401	4400	4400

The first fundamental overtone of the OH stretching vibrations of layered silicate is in the range 7160–7300  $\text{cm}^{-1}$  (Figure 5c). The statistics and assignments of the peaks are presented in Table 4. The weak interlayer water peaks were excluded. There are two strong peaks at 7170 and 7240  $\text{cm}^{-1}$  in the lizardite spectra. Chrysotile only has a strong peak at 7233  $\text{cm}^{-1}$ , a weak shoulder peak at 7234  $\text{cm}^{-1}$ , and very weak peak at 7170  $\text{cm}^{-1}$ . Antigorite has a strongest peak at 7231  $\text{cm}^{-1}$  and a clear peak at 7243  $\text{cm}^{-1}$ . It is not accurate to judge the existence of chrysotile solely on whether there is strip near 7233  $\text{cm}^{-1}$  [25].

**Table 4.** The bands in the range 7000–7600  $\text{cm}^{-1}$  for the related samples (in  $\text{cm}^{-1}$ ).

Outer OH	DWH14-lz	ZH41-lz	Z3-lz	SZ17-lz	SM-ctl	H7-atg	H11-atg
$\nu_{\text{OH-s}}$	7170	7168	7170	7167	7170	7168	7167
$\nu_{\text{OH-s}} +$	7204	7203	7204	7204	7204	7204	7203
$\nu_{\text{OH-v}}$	7234	7233	7233	7231	7233	7231	7230
$\nu_{\text{OH-v}}$	7241	7241	7242	7241	7243	7243	7241

#### 4. Discussion

The band frequency relationships between the MIR and NIR spectra were determined via trial-and-error summations. Post [15] pointed out that there are two theories regarding the assignment of the peak at  $4300\text{ cm}^{-1}$ . The stretching vibrations of the inner OH and outer OH are combined with different OH bending vibrations [18,26,27]. However, according to Bishop [17], peaks at  $4280$  and  $4300\text{ cm}^{-1}$  correspond to the combination of the internal or external hydroxyl stretching vibration and the bending vibration of the same hydroxyl group, and the peak at  $4315\text{ cm}^{-1}$  has not been analyzed. Combined with the data obtained in our experiment, we determined a more suitable peak assignment: the absorption band at  $4280\text{ cm}^{-1}$  was attributed to the combination of the  $3650\text{ cm}^{-1}$  assigned outer OH sloping stretching vibration and the  $630\text{ cm}^{-1}$  assigned antisymmetric OH-Mg-OH translation vibration. Additionally, the band at  $4300\text{ cm}^{-1}$  was attributed to the combination of the  $3690\text{ cm}^{-1}$  assigned outer OH sloping stretching vibration and the  $610\text{ cm}^{-1}$  assigned antisymmetric OH-Mg-OH translation vibration. The specific corresponding values of the three serpentine minerals are shown in Table 5. The outer OH sloping stretching vibration of H7-atg and H11-atg participates in the combination as a whole and the average value of  $3643\text{ cm}^{-1}$  has good results. All of the errors are within  $10\text{ cm}^{-1}$  [28]. The peak at  $4279\text{ cm}^{-1}$  is not obvious due to the weak OH sloping stretching vibration in antigorite. The combination of  $3674\text{ cm}^{-1}$  assigned to the outer OH vertical stretching vibration, with  $620\text{ cm}^{-1}$  assigned to the antisymmetric OH-Mg-OH translation vibration, is strong and clear. The  $3674\text{ cm}^{-1}$  peak also combines with the  $645\text{ cm}^{-1}$  peak assigned to the antisymmetric OH-Mg-OH translation vibration, presenting as a shoulder peak at  $4315\text{ cm}^{-1}$ . In the other two kinds of serpentines, the peak intensity at  $648\text{ cm}^{-1}$  is weak, so the  $4315\text{ cm}^{-1}$  peak is difficult to observe. All of the samples exhibit an obvious peak near  $4400\text{ cm}^{-1}$ . Bishop [24] believes that  $\text{Fe}^{3+}$  replaces Mg and that the formation of  $\text{Fe}^{3+}\text{Mg}_2\text{-OH}$  causes this peak, which demonstrates that the substitution of Fe for Mg in the octahedral layer is common in serpentine.

The OH group vibration of serpentine in the mid-infrared region corresponds to the first fundamental overtone of the OH group stretching vibrations in the near-infrared range. The specific corresponding values of the three types of serpentines are presented in Table 6. The peak near  $7170\text{ cm}^{-1}$  belongs to the overtone of the outer OH sloping stretching vibration near  $3648\text{ cm}^{-1}$ . The peak near  $7204\text{ cm}^{-1}$  belongs to the overtone of the combination of the outer OH sloping and vertical stretching vibrations near  $3648$  and  $3689\text{ cm}^{-1}$ . The peaks near  $7233$  and  $7241\text{ cm}^{-1}$  belong to the overtone of the outer OH vertical stretching vibration. The outer OH sloping stretching vibration of antigorite also participates in the overtone as a whole.

The overtone of the vertical stretching vibration of the inner OH group should be around  $7273\text{ cm}^{-1}$ , but there is no absorption in the spectrum at this position. It is possible that the vibrating direction of the OH group is limited, and thus the overtone vibrations cancel each other.

Due to the non-ideality of the structure and composition, the average factor between the OH stretching vibration and its overtone is  $1.965 (+0.0026, -0.0037)$  rather than 2, which is consistent with Bishop [17] but more accurate. Among the samples, the average factor of samples from the Hanzhong area is less than 1.965, while the average factor of samples from the Xiuyan area is greater than 1.965, which may be used as the basis for origin differentiation, although future experiments with more samples will be required to confirm.

**Table 5.** The major NIR bands in the range 4000–4600 cm<sup>-1</sup> related to the serpentine samples and their corresponding MIR peaks (in cm<sup>-1</sup>).

	Lizardite					Chrysotile					Antigorite			
	Measured Peak	Fundamental Peaks	Theoretical Peak	Δ		Measured Peak	Fundamental Peaks	Theoretical Peak	Δ		Measured Peak	Fundamental Peaks	Theoretical Peak	Δ
DWH14-lz	4281	3650 + 630	4280	1	SM-ctl	4279	3648 + 629	4277	2	H7-atg	4279	3643 * + 645	4288	9
	4301	3689 + 609	4298	3		4304	3689 + 609	4298	6		4302	3674 + 621	4295	7
ZH41-lz	4281	3647 + 630	4277	4						H11-atg	4315	3674 + 645	4319	4
	4301	3688 + 609	4297	4							4279	3643 * + 644	4288	9
Z3-lz	4281	3649 + 629	4278	3							4301	3674 + 619	4295	6
	4301	3688 + 609	4297	4							4315	3674 + 644	4319	4
SZ17-lz	4281	3648 + 630	4278	3										
	4301	3688 + 610	4298	3										

\* Antigorite: 3643 = (3632 + 3654)/2, the peaks at 3632 and 3654 cm<sup>-1</sup> are all due to the outer OH sloping stretching vibration.

**Table 6.** The major NIR bands in the range 7000–7600 cm<sup>-1</sup> related to the serpentine samples and their corresponding MIR peaks (in cm<sup>-1</sup>).

	Lizardite				Chrysotile				Antigorite		
	Measured Peak	Fundamental Peaks	Factor		Measured peak	Fundamental Peaks	Factor		Measured Peak	Fundamental Peaks	Factor
DWH14-lz	7170	3650	1.9644	SM-ctl	7170	3648	1.9655	H7-atg	7168	3643 *	1.9676
	7204	(3650 + 3689)/2	1.9632		7204	(3648 + 3689)/2	1.9637		7204	(3643 * + 3693)/2	1.9640
	7234	(3678 + 3689)/2	1.9639		7233	(3668 + 3689)/2	1.9663		7231	(3674 + 3693)/2	1.9631
	7241	3689	1.9629		7243	3689	1.9634		7243	3693	1.9613
ZH41-lz	7168	3647	1.9655					H11-atg	7167	3643 *	1.9673
	7203	(3647 + 3688)/2	1.9640						7203	(3643 * + 3696)/2	1.9629
	7233	(3665 + 3688)/2	1.9674						7230	(3674 + 3696)/2	1.9673
	7241	3688	1.9634						7241	3696	1.9673
Z3-lz	7170	3649	1.9649								
	7204	(3649 + 3688)/2	1.9637								
	7233	(3670 + 3688)/2	1.9660								
	7242	3688	1.9637								
SZ17-lz	7167	3648	1.9646								
	7204	(3648 + 3688)/2	1.9640								
	7231	(3667 + 3688)/2	1.9663								
	7241	3688	1.9634								
		Average				Average					Average
		1.9645				1.9647					1.9651

\* Antigorite: 3643 = (3632+3654)/2, the peaks at 3632 and 3654 cm<sup>-1</sup> are all due to the outer OH sloping stretching vibration.

## 5. Conclusions

1. There are obvious differences in the infrared spectrum of the three serpentine minerals. Lizardite has two equal-height peaks at 4280 and 4300  $\text{cm}^{-1}$ , and two strong peaks at 7170 and 7241  $\text{cm}^{-1}$ . Chrysotile has a shoulder peak at 4280  $\text{cm}^{-1}$  and 7243  $\text{cm}^{-1}$  and only one strong peak at 7233  $\text{cm}^{-1}$ . There are single strong peaks at 3674  $\text{cm}^{-1}$ , 4300  $\text{cm}^{-1}$ , and 7231  $\text{cm}^{-1}$  and weak shoulder peaks at 4280  $\text{cm}^{-1}$  and 4315  $\text{cm}^{-1}$  for antigorite, with a clear peak at 7242  $\text{cm}^{-1}$ . These characteristic peaks are helpful in identifying and distinguishing between serpentine minerals.
2. In the range 4000–4600  $\text{cm}^{-1}$ , the serpentine peaks correspond to the OH secondary combination band region and in the range between 4280 and 4300  $\text{cm}^{-1}$ , it corresponds to a combination of sloping, vertical stretching, and bending vibrations of the outer OH groups. The 7000–7600  $\text{cm}^{-1}$  band is the first fundamental overtone of the OH group stretching vibrations. The peaks at 7170, 7204, 7233, and 7242  $\text{cm}^{-1}$  correspond to the overtone of the sloping stretching vibration of the outer OH group, the overtone combined sloping stretching vibration and vertical stretching vibration of the outer OH group, and the overtone of the vertical stretching vibration of the outer OH group, respectively.
3. Due to the non-ideal conditions, the actual position of the overtone peak is lower than the theoretical position. The factor of the first fundamental overtone of the OH group stretching vibration is about 1.965.

**Author Contributions:** Conceptualization, M.H.; Data curation, S.W. and B.Z.; Formal analysis, S.W., M.Y. and B.Z.; Funding acquisition, F.W. and Q.L.; Investigation, Q.L.; Methodology, S.W. and M.Y.; Project administration, M.H.; Resources, F.W. and Q.L.; Writing—original draft, S.W. and B.Z.; Writing—review & editing, M.H. and M.Y. All authors have read and agreed to the published version of the manuscript.

**Funding:** National Mineral Rock and Fossil Specimens Resource Center.

**Data Availability Statement:** Not applicable.

**Conflicts of Interest:** The authors declare no conflict of interest.

## References

1. Yu, X.Y. *Colored Gemmology*, 2nd ed.; Geological Publishing House: Beijing, China, 2009; pp. 86–87.
2. Salzer, R. Practical Guide to Interpretive Near-Infrared Spectroscopy. By Jerry Workman, Jr. and Lois Weyer. *Angew. Chem. Int. Ed.* **2008**, *47*, 25. [[CrossRef](#)]
3. Li, Y.Q.; Jiang, S.Y.; Fan, W.W. Study on the Infrared Spectra of Chrysotiles in China. *Chin. J. Geol.* **1981**, *3*, 247–253.
4. Xu, G.T.; Yuan, H.F.; Lu, W.Z. Development of Modern Near Infrared Spectroscopic Techniques and Its Applications. *Spectrosc. Spectr. Anal.* **2000**, *2*, 134–142.
5. Chu, X.L.; Yuan, H.F.; Lu, W.Z. Progress and Application of Spectral Data Pretreatment and Wavelength Selection Methods in NIR Analytical Technique. *Anal. Instrum.* **2006**, *2*, 1–10.
6. Zheng, A.B.; Yang, H.H.; Pan, X.P.; Yin, L.H.; Feng, Y.C. Identifying Multi-Class Drugs by Using Near-Infrared Spectroscopy and Variational Auto-Encoding Modeling. *Spectrosc. Spectr. Anal.* **2020**, *40*, 3946–3952.
7. Petriglieri, J.R.; Salvioli-Mariani, E.; Mantovani, L.; Tribaudino, M.; Lottici, P.P.; Laporte-Magoni, C.; Bersani, D. Micro-Raman mapping of the polymorphs of serpentine. *J. Raman Spectrosc.* **2015**, *46*, 953–958. [[CrossRef](#)]
8. Groppo, C.; Rinaudo, C.; Cairo, S.; Gastaldi, D.; Compagnoni, R. Micro-Raman spectroscopy for a quick and reliable identification of serpentine minerals from ultramafics. *Eur. J. Mineral.* **2006**, *18*, 319–329. [[CrossRef](#)]
9. Farmer, V.C. *The Infrared Spectra Of Minerals*; The Mineralogical Society of Great Britain & Ireland: Middlesex, UK, 1974; p. 539.
10. Cheng, H.F.; Hao, R.W.; Zhou, Y. Visible and near-infrared spectroscopic comparison of five phyllosilicate mineral samples. *Spectrochim. Acta Part A Mol. Biomol. Spectrosc.* **2017**, *180*, 19–22. [[CrossRef](#)] [[PubMed](#)]
11. Li, X.J.; Yu, L.; Zu, E.D. Application of Near Infrared Spectroscopy in the Study of Gems. *Spectrosc. Spectr. Anal.* **2018**, *38*, 54–57.
12. Zhang, S.J.; Deji, Z.; Qin, H.; Liu, H.; Luosang, D.; Cheng, H.F. The Structure of Layered Silicate Mineral and Their Vibrational Spectra Characteristics. *China Non-Met. Miner. Ind.* **2018**, *2*, 1–7.
13. Yariv, S. Infrared evidence for the occurrence of SiO groups with double-bond character in antigorite, sepiolite and palygorskite. *Clay Miner.* **1986**, *21*, 925–936. [[CrossRef](#)]
14. Klopogge, J.T.; Frost, R.L.; Rintoul, L. Single crystal Raman microscopic study of the asbestos mineral chrysotile. *Phys. Chem. Chem. Phys.* **1999**, *1*, 2559–2564. [[CrossRef](#)]

15. Post, J.L.; Borer, L. High-resolution infrared spectra, physical properties, and micromorphology of serpentines. *Appl. Clay Sci.* **2000**, *16*, 73–85. [[CrossRef](#)]
16. Trittschack, R.; Grobéty, B.; Koch-Müller, M. In situ high-temperature Raman and FTIR spectroscopy of the phase transformation of lizardite. *Am. Mineral.* **2012**, *97*, 1965–1976. [[CrossRef](#)]
17. Bishop, J.; Murad, E.; Dyar, M.D. The influence of octahedral and tetrahedral cation substitution on the structure of smectites and serpentines as observed through infrared spectroscopy. *Clay Miner.* **2002**, *37*, 617–628. [[CrossRef](#)]
18. Uehara, S.; Shirozu, H. Variations in chemical composition and structural properties of antigorites. *Mineral. J.* **1985**, *12*, 299–318. [[CrossRef](#)]
19. Luce, R.W. Identification of serpentine varieties by infrared absorption. *Geol. Sur. Prof. Pap.* **1971**, *750*, 199–201.
20. Rinaudo, C.; Gastaldl, D.; Belluso, E. Characterization of Chrysotile, Antigorite and Lizardite by FT-Raman Spectroscopy. *Can. Mineral.* **2003**, *41*, 883–890. [[CrossRef](#)]
21. Xue, L.; Wang, Y.Q.; Fan, J.L. Study on the Spectroscopy of Yellow Serpentine Jade. *Laser Infrared* **2009**, *39*, 267–270.
22. Prencipe, M.; Noel, Y.; Marco Bruno, M.; Dovesi, R. The vibrational spectrum of lizardite-1T [Mg<sub>3</sub>Si<sub>2</sub>O<sub>5</sub>(OH)<sub>4</sub>] at the  $\Gamma$  point: A contribution from an ab initio periodic B3LYP calculation. *Am. Mineral.* **2015**, *94*, 986–994. [[CrossRef](#)]
23. Balan, E.; Saitta, A.M.; Mauri, F.; Lemaire, C.; Guyot, F. First-principles calculation of the infrared spectrum of lizardite. *Am. Mineral.* **2015**, *87*, 1286–1290. [[CrossRef](#)]
24. Bishop, J.L.; Lane, M.D.; Dyar, M.D.; Brown, A.J. Reflectance and emission spectroscopy study of four groups of phyllosilicates: Smectites, kaolinite-serpentines, chlorites and micas. *Clay Miner.* **2008**, *43*, 35–54. [[CrossRef](#)]
25. Jana Madejová, J.; Jankovič, L.; Pentrák, M.; Komadel, P. Benefits of near-infrared spectroscopy for characterization of selected organo-montmorillonites. *Vib. Spectrosc.* **2011**, *57*, 8–14. [[CrossRef](#)]
26. Hunt, G.R.; Ashley, R.P. Spectra of altered rocks in the visible and near infrared. *Econ. Geol.* **1979**, *74*, 1613–1629. [[CrossRef](#)]
27. King, T.V.; Clark, R.N. Spectral characteristics of chlorites and Mg-serpentines using high-resolution reflectance spectroscopy. *J. Geophys. Res. Solid Earth* **1989**, *94*, 13997–14008. [[CrossRef](#)]
28. Baron, F.; Petit, S. Interpretation of the infrared spectra of the lizardite-nepouite series in the near- and mid-infrared range. *Am. Mineral.* **2016**, *101*, 423–430. [[CrossRef](#)]